

RELATIVISTIC MERGERS OF BLACK HOLE BINARIES
HAVE LARGE, SIMILAR MASSES, LOW SPINS AND ARE CIRCULARPAU AMARO-SEOANE¹ & XIAN CHEN²(Dated: March 1, 2016)
Draft version March 1, 2016

ABSTRACT

Gravitational waves are a prediction of general relativity, and with ground-based detectors now running in their advanced configuration, we will soon be able to measure them directly for the first time. Binaries of stellar-mass black holes are among the most interesting sources for these detectors. Unfortunately, the many different parameters associated with the problem make it difficult to promptly produce a large set of waveforms for the search in the data stream. To reduce the number of templates to develop, one must restrict some of the physical parameters to a certain range of values predicted by either (electromagnetic) observations or theoretical modeling. In this work we show that “hyperstellar” black holes (HSBs) with masses $30 \lesssim M_{\text{BH}}/M_{\odot} \lesssim 100$, i.e. black holes significantly larger than the nominal $10M_{\odot}$, will have an associated low value for the spin, i.e. $a < 0.5$. We prove that this is true regardless of the formation channel, and that when two HSBs build a binary, each of the spin magnitudes is also low, and the binary members have similar masses. We also address the distribution of the eccentricities of HSB binaries in dense stellar systems using a large suite of three-body scattering experiments that include binary-single interactions and long-lived hierarchical systems with a highly accurate integrator, including relativistic corrections up to $\mathcal{O}(1/c^5)$. We find that most sources in the detector band will have nearly zero eccentricities. This correlation between large, similar masses, low spin and low eccentricity will help to accelerate the searches for gravitational-wave signals.

Subject headings: gravitational waves — relativistic processes — stars: black holes — stars: kinematics and dynamics

1. INTRODUCTION

The first-generation ground-based detector Laser Interferometer Gravitational-wave Observatory (LIGO) has successfully undergone major technical upgrades in the past few years that have led to a significant increase of the volume of the observable universe³. The detector has already been operative for a few months and *observation run 1* (O1) is being analyzed as these lines are written. In this configuration, LIGO can observe binaries of stellar-mass black holes (BHs)—one of the most interesting sources to be detected—of masses $(25+25)M_{\odot}$ out to a distance of ~ 3.4 Gpc (a redshift of $z \sim 0.2-0.3$), and with the final advanced (aLIGO) configuration about a factor 3 farther away (see Brown et al. 2013 and LIGO Scientific Collaboration et al. 2013). On the other hand, the Virgo Interferometer⁴ is currently undergoing an upgrade program to improve its strain sensitivity, and will be online in the advanced configuration in the next future. The first direct detection of GWs is imminent, provided the number of sources in the observable volume of aLIGO is big enough.

The fundamental low-frequency limitations of the second-generation detectors are given by thermal, gravity gradient, and seismic noise. To circumvent these problems, yet a third generation of gravitational-wave (GW) interferometers to be operated underground is currently being proposed. The Einstein Telescope⁵ will be a 10 km laser-interferometer with a

sensitivity 100 times better than that of the current detectors, which expands the observable volume of the universe by a factor of a million (Sathyaprakash et al. 2010). Moreover it will cover the frequency range between 1 Hz and 10^4 Hz.

For the search, the availability of accurate waveform models for the full merger is pivotal. Numerical relativity succeeded ten years ago in simulating the late inspiral, merger and ringdown (Pretorius 2005; Campanelli et al. 2006; Baker et al. 2006). Together with post-Newtonian modeling of the inspiral phase, data analysts can do faithful searches for binaries of BHs of comparable-mass and with mass ratios up to about 10 (see e.g. Buonanno & Damour 1999; Buonanno et al. 2007; Ajith et al. 2009; Santamaría et al. 2010). Nonetheless, the high cost of the development of the many ($\sim 10^5 - 10^6$) waveforms necessary for a matched-filtering search represents a problem, if not a true limitation.

Hence, to speed up the production of waveforms, certain values are assumed for some of the physical parameters. These values are not chosen randomly, but rely on electromagnetic observations or theoretical modeling, which represents an emergent symbiotic relationship between astrophysics and GW searches—we reduce the spectrum of the parameter space based on our best understanding of the astrophysics of the system and, once the first detections arrive, they will help us to understand our astrophysical models better.

Following this line of thought, in this paper we show that there is a correlation between the mass of BHs with large masses, which we call “hyperstellar” (henceforth HSB)⁶, and

¹ Max Planck Institut für Gravitationsphysik (Albert-Einstein-Institut), D-14476 Potsdam, Germany

² xchen@astro.puc.cl, Instituto de Astrofísica, Facultad de Física, Pontificia Universidad Católica de Chile, 782-0436 Santiago, Chile

³ <http://www.ligo.caltech.edu/advLIGO/>

⁴ <http://www.virgo-gw.eu/>

⁵ <http://www.et-gw.eu/>

⁶ Depending on the mass, a BH is (a) supermassive ($\gtrsim 10^6 M_{\odot}$), (b) stellar-mass ($\sim 10 M_{\odot}$) or (c) intermediate-massive (IMBH, $[100, 10^5] M_{\odot}$). The range of masses we are interested in is $20 \lesssim M_{\text{BH}}/M_{\odot} \lesssim 100$. Since these BHs are too heavy compared to

their spin. HSBs are expected to form in low-metallicity environments following the collapse of very-massive stars, as in the works of Woosley et al. (2002); Heger et al. (2003), and have been suggested to be the central engines of those ultra-luminous X-ray sources found in star-forming galaxies (Mapelli et al. 2009, 2010; Mapelli & Zampieri 2014, who call this sort of BHs “massive stellar black holes”). *We show that BHs with masses $\gtrsim 30 M_\odot$ will be detected with typically low spin values ($\lesssim 0.50$) and on basically circular binary orbits.*

2. BINARIES OF HYPERSTELLAR BLACK HOLES

Binaries of compact objects in the relativistic regime detectable by ground-based interferometers like aLIGO can, in principle, form in two different ways (see e.g. the Living Review paper by Benacquista & Downing 2013 and references therein): (i) in galactic plane or bulge as the remnants of massive binary stars (“field binaries”), or (ii) in dense stellar systems, such as globular and young clusters, or those nuclear star clusters at the centers of galaxies, via dynamical interactions (henceforth “dynamical binaries”).

2.1. Field binaries

To have two BHs in a field binary, we need a binary formed of two stars that are both massive enough (e.g. de Mink & Belczynski 2015). Since we need them bound, the natal kick that the BHs receive during their formation cannot exceed the break-up velocity of the stellar binary. This favors the formation of binaries of HSBs because (i) high-mass BHs receive relatively small natal kicks (Belczynski et al. 2015) and (ii) a higher mass requires a larger break-up velocity. For these reasons, we expect the ground-based GW experiments to detect mostly HSBs (see Dominik et al. 2015, for a more quantitative evaluation).

2.2. Dynamical binaries

Dynamical binaries will naturally tend to form with large masses. This is so because the timescale for an object to sink towards the center of a stellar system via dynamical friction is the relaxation time divided by its mass – more massive stars will sink first into a dense environment. Moreover, binaries of larger masses are more difficult to separate in three-body interactions because of the larger binding energy.

In particular, O’Leary et al. (2006a) found with Monte-Carlo simulations BH masses well exceeding the nominal $10 M_\odot$ in (20–80)% of the binaries in globular clusters, and Miller & Lauburg (2009) estimated with semi-analytical arguments and scattering experiments that there is a strong tendency for the merging BHs in nuclear star clusters to be biased toward high masses.

This bias of forming massive binaries due to the existence of HSBs has been confirmed using direct-summation N -body simulations of young clusters (Mapelli et al. 2013). As a result of the above bias, ground-based observatories are more likely to detect HSB binaries in dense clusters than in the stellar-mass range (i.e. with masses of about $10 M_\odot$ O’Leary et al. 2006b; Miller & Lauburg 2009; Ziosi et al. 2014; Rodriguez et al. 2015).

3. ESTIMATION OF THE SPIN FOR FIELD HSB BINARIES

the nominal mass of an stellar-mass BH but well below the mass of an IMBH, we choose the name “hyperstellar” to avoid confusion.

In the field, the only way to produce a HSB binary is to form, in the first place, a stellar binary of two Wolf-Rayet (WR) stars (with stellar mass $M_* > 60 M_\odot$, following the definition of Zinnecker & Yorke 2007). An environment with low metallicity is more favorable. For example, in a solar-metallicity environment, a $80 M_\odot$ WR star produces a BH of only $10 M_\odot$ (Woosley et al. 2002), but in an environment with 0.1 solar metallicity the same star can produce a $30 M_\odot$ HSB (e.g. Dominik et al. 2015). It is interesting to note that for extremely metal-poor environments (which are uncommon in the redshift range of our interest, $z \lesssim 0.2 - 0.3$, Panter et al. 2008), HSBs in the mass range $25 - 55 M_\odot$ are prevented from forming because of a pair-instability process during the supernova phase (Heger et al. 2003; Fryer et al. 2012).

Because of angular-momentum loss by stellar wind, WR stars are slow rotators. The rotational velocity at the stellar surface drops from an initial value of $200 - 300 \text{ km s}^{-1}$ to below 50 km s^{-1} during the stellar evolution (Meynet & Maeder 2003, 2005). As a result, the compact remnant which is sitting at the core of a WR star retains very little of the initial angular momentum. For example, when $M_* = 80 M_\odot$ —which is the initial stellar mass relevant to HSB formation—the current stellar evolution models predict that the specific angular momentum measured at the edge of the stellar remnant will drop from $\sim 10^{18} \text{ cm}^2 \text{ s}^{-1}$ in the initial configuration to as small as $j_{\text{rem}} \simeq (1 - 6) \times 10^{16} \text{ cm}^2 \text{ s}^{-1}$, and even smaller for more massive stars (Hirschi et al. 2005; Yusof et al. 2013).

Since the remnant of a WR star has a low specific angular momentum, the HSB must be a slow rotator. Even under the assumption that no angular momentum is lost during the collapse of the remnant and the growing of the initial seed BH that eventually becomes a HSB, the spin parameter of the final HSB is:

$$a = \frac{j_{\text{rem}} M_\bullet}{GM_\bullet^2/c} \simeq (0.075 - 0.45) \left(\frac{M_\bullet}{30 M_\odot} \right)^{-1}, \quad (1)$$

where c is the speed of light. Note that because of the reason we just argued, this is an upper limit, and in a more realistic estimation, the value will be even lower. Also, it is interesting to note that Equation (1) gives the same spin range as what we have observed currently for the stellar-mass BHs ($M_\bullet < 20 M_\odot$) in the Local Group (McClintock et al. 2014).

To spin up the slowly rotating HSB that we have predicted, the only two possibilities are (i) merger with another HSB because of a dynamical interaction, such as a three-body encounter, or (ii) accretion of enough material onto the HSB, about an amount of M_\bullet to achieve a result of $a > 0.5$. The first possibility can indeed enhance the spin value of the merger product to $a > 0.5$. However, this process cannot take place in the field, because the stellar relaxation timescale (i.e. encounter timescale) exceeds by many orders of magnitude the Hubble time. Moreover, in the next section we will see that the outcome will not be observed because of a dynamical selection effect.

Regarding (ii), there are two sources that can possibly provide material to feed the HSB, either the interstellar medium (ISM) surrounding our field binary, or the companion star, i.e. the other WR star in the binary which may not have collapsed into a BH yet. The Bondi-Hoyle accretion rate from the ISM is $10^{-15} M_\odot \text{ yr}^{-1} (\sigma/10^2 \text{ km s}^{-1}) (n_{\text{ISM}}/1 \text{ cm}^{-3}) (M_\bullet/30 M_\odot)^2$ where n_{ISM} is the proton density in ISM and σ the velocity dispersion of stars (Miller & Lauburg 2009). This feeding

rate is too low to spin up the HSB, because it would require a time longer than the Hubble time. On the other hand, the life span of the WR companion star is of 5 Myr, which is too short compared to the minimum timescale for a BH to double its mass by accreting at the maximum (Eddington) rate. This is the Salpeter timescale, which is about 30 Myr assuming that 10% of the rest mass is converted into radiation (see Sec. 6.3 in McClintock et al. 2014).

We hence deduce that *field HSBs must be slow rotators, with lower values than the upper limit shown in Eq. 1 because of loss of angular momentum during the remnant collapse.*

4. ESTIMATION OF THE SPIN FOR DYNAMICAL HSB BINARIES

For this section, we assume that the HSB binary forms dynamically from two HSBs that were born isolated (if this is not the case, then the previous result applies) and then later formed a binary via three-body interactions.

There are three possible channels to form an isolated HSB: (i) The collapse of an isolated WR star, (ii) the coalescence of two less massive BHs (e.g. $10 < (M_\bullet/M_\odot) < 30$) and (iii) by accreting background stars.

Channel (i): As we have seen in Section 3, HSBs with masses higher than $30 M_\odot$ have typically low spins, $a < 0.5$. This HSB receives a natal kick typically of $15[M_\bullet/(30 M_\odot)]^{-1} \text{ km s}^{-1}$ (Belczynski et al. 2015) and is hence kept in the host cluster, because the velocity dispersion is of order 10 km s^{-1} . Lighter BHs will not be retained. Since we want to build binaries, it is important to retain them in the cluster. Hence, most BHs with masses lighter than $30 M_\odot$ are typically bound to leave the cluster at birth, without a chance of forming a binary.

Channel (ii): Although we have just shown that lighter BHs typically abandon the host cluster at birth, there is sufficient margin so that some remain (see e.g. the work of Strader et al. 2012, although the accretion rate is so low that it is difficult to assess whether the BHs are 10 or $20 M_\odot$), and so we also address this channel. We point out two particular properties of dynamical binaries that will be important in determining the spin parameter, a_{fin} , of the final merged BH. (a) On average, the two members of a dynamical BH binary very likely will have similar masses because the three-body interaction tends to retain equal-mass binaries. This is particularly true for BHs, since they belong to the heaviest objects in clusters, and so they have lower probabilities to be ionized or replaced by another interloper (see e.g. Miller & Lauburg 2009). (b) The majority of BH-BH mergers have a zero-eccentricity orbit, as we will see in Section 5. As a result of these two points, the binary has a significant amount of angular momentum before it merges, and hence preferentially produces a high-spin HSB by the end of the merger.

To prove this, we calculate the distribution of a_{fin} for different mass ratios ($q := m_2/m_1$, with m_1 the more massive BH), using the method developed by one of us and presented in Liu et al. (2012). The algorithm chooses a random orientation for the spin axis of each progenitor, and then, given the mass ratio q ($q \leq 1$ in our model) of the two BHs, computes a_{fin} and the relativistic recoiling velocity, v_k , according to the empirical fitting formulae derived from numerical relativity simulations (Rezzolla et al. 2008; Baker et al. 2008; van Meter et al. 2010).

The top panel of Figure 1 shows our results, where we have assumed a random distribution for the spin magnitudes in the range $[0, 0.9]$ for the two progenitors. We can see that when $q > 0.2$, the value of a_{fin} is most likely greater than 0.4, which correlates into a very large relativistic recoiling velocity (see

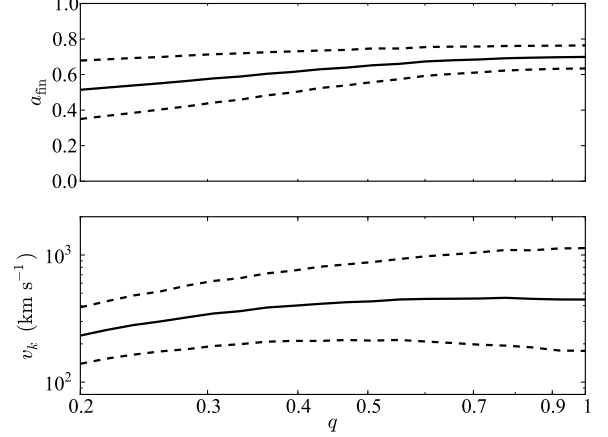


FIG. 1.— Distributions of the final spin a_{fin} (upper panel) and recoiling velocity v_k (lower panel) of a post-merger BH as a function of the mass ratio of q the two BH progenitors. The solid lines show the mean value and the dashed ones the 1σ range. To derive these distributions, we run for each q value a Monte-Carlo simulation of 4000 trials, each trial starting with random spin magnitude (between 0 and 0.9) and orientation for each of the two BH progenitors.

lower panel of Fig. 1), that, for all purposes, is much higher than the average dispersion velocity of the host cluster, typically of 10 km s^{-1} . The excess of recoiling velocity relative to the velocity dispersion of the host stellar system is also true even for Nuclear Star Clusters (NSC, dense stellar clusters found at the center of galaxies of all Hubble types, see e.g. Böker 2010), whose dispersion velocities are around $\sigma \sim 50 \text{ km s}^{-1}$, see e.g. Miller & Lauburg 2009.

Hence, even if the few remaining lighter BHs led to the formation of high-spin HSBs in clusters, these are immediately kicked out of the host environment because of the relativistic kick, and do not stand a chance of forming a binary.

Channel (iii): By accreting background stars, a BH with a mass initially well below $30 M_\odot$ cannot become a HSB. This is because the accretion rate from other stars in a very dense environment, such as a NSC, is

$$\begin{aligned} \Gamma &\simeq n_* \sigma r_t^2 \left(1 + \frac{2GM_\bullet}{r_t \sigma^2}\right) \\ &\simeq 8.6 \times 10^{-11} \text{ yr}^{-1} \left(\frac{n_*}{10^6 \text{ pc}^{-3}}\right) \left(\frac{\sigma}{50 \text{ km/s}}\right)^{-1} \left(\frac{M_\bullet}{10 M_\odot}\right)^{4/3}, \end{aligned} \quad (2)$$

where $r_t \simeq R_\odot (M_\bullet/M_\odot)^{1/3}$ is the critical radius for the BH to tidally disrupt a solar-type star and n_* is the spatial density of background stars. Hence, in this channel we cannot form HSBs.

Therefore HSBs retained in globular clusters or NSC predominantly have slow spin ($a_\bullet < 0.5$), and hence *dynamical BH binaries detected with ground-based detectors will be HSBs with low spin.*

5. ECCENTRICITY DISTRIBUTION

Field binaries will have low eccentricities when they enter the detector band because their orbits circularize during the binary-star evolution due to Roche lobe overflow, common envelope phase and tidal synchronization (see e.g. Belczynski et al. 2008; de Mink & Belczynski 2015) and, much later

in the evolution, due to GW radiation. For dynamical binaries, however, the eccentricities in the detector band are more uncertain, because of dynamical interactions with other stars. For instance, a binary-binary interaction can lead to the existence of a third body gravitationally bound to and interacting with the binary (though the probability to form a triple via single-binary interaction is very low, at least for bodies with the same masses, see Miller & Hamilton 2002 and references therein). For this particular situation, the interaction can lead to a large oscillation of the orbital eccentricity of the binary because of the Kozai-Lidov resonance (see e.g. Blaes et al. 2002). In this case, as many as 50% of mergers in the detector band could have an eccentricity larger than $e = 0.1$ (Wen 2003; Antonini et al. 2014, 2015). These results hold for bound triple systems in which all bodies have a similar or equal mass in the stellar-mass BH range (i.e. around $10M_\odot$). However, direct-summation N -body simulations that do not make a priori assumptions about mass ratios and bound systems, find that BH-BH mergers are preferentially circular ($e < 0.1$) and driven by interactions with unbound small bodies (which is referred to as hardening in stellar dynamics) (Ziosi et al. 2014). Unfortunately, such direct-summation simulations are very expensive and not suited for statistical studies.

Hence, to statistically address the evolution of the eccentricities of the HSB binaries during three-body interactions, we use the numerical tool FEWBODY (Fregeau et al. 2004; Fregeau & Rappaport 2004). Moreover, we have modified it by adding relativistic corrections to the force term, which might be important in the kind of interactions that we are interested in (HSB binaries). For this, we have chosen the centre-of-mass frame of the binary for the post-Newtonian (PN hereafter) expressions, which is equivalent to the center-of-mass Hamiltonian in ADM (Arnowit, Deser and Misner) coordinates thanks to a transformation of the particles' variables, following the expressions given by Blanchet & Iyer (2003). This means that the relative acceleration in the center-of-mass frame has the form

$$\frac{dv^i}{dt} = -\frac{m}{r^2} \left[(1 + \mathcal{A})n^i + \mathcal{B}v^i \right] + \mathcal{O}\left(\frac{1}{c^7}\right), \quad (3)$$

where the relative separation of the binary is $x^i = y_1^i - y_2^i$, $r = |\mathbf{x}|$ and $n^i = x^i/r$; the \mathcal{A} and \mathcal{B} are given by the expressions (3.10a) and (3.10b) in Blanchet & Iyer (2003). We truncate the series and neglect all terms of order higher than 2.5 PN, since e.g. the 3 PN correction requires a very expensive computation and provides us only with a correction which is negligible for the purpose of this study. On the other hand, the 3.5 PN term, even if it is significantly less challenging, would provide us only with a rough ($\sim 10\%$) estimate of the gravitational recoil velocity. In other words, we focus in this work only on the relativistic corrections corresponding to periastron shift (1 PN and 2 PN) and the energy loss in the form of GW radiation (2.5 PN). The first implementation of relativistic terms in a dynamical code was done by one of us and they have been well tested in a number of different works that feature different orders in the expansion (see e.g. Kupi et al. 2006; Amaro-Seoane et al. 2012; Brem et al. 2013, 2014; Antognini et al. 2014).

The initial conditions for all experiments are a binary of two HSBs plus an unbound interloper. We note that during the interactions, there are long-lived hierarchical triples forming, which are hence also included in the experiments. We assume a relative velocity corresponding to the velocity dis-

tribution of a NSC, 50 km s^{-1} . Initially the code calculates b_0 , the impact parameter corresponding to a classical, point-mass closest approach of $2a$. It then performs scattering experiments with b increasing from near zero, following a distribution uniform in area, $dN/db \propto b$. It continues performing classical, point-mass closest approach of $2a_0$, where a_0 is the initial semimajor axis of the HSB binary. It then performs scattering experiments with b increasing from near zero. It continues performing experiments as long as b is less than b_0 , or b is less than two times the last b for which the encounter was either a recordable event or a resonant encounter. The reason for the latter constraint on b is to ensure that any interesting encounters that might occur at large b are not missed. The masses of the HSBs are set to $m_1 = m_2 = 30M_\odot$. In a dense stellar environment such as a NSC, a BH binary becomes hard when its kinetic energy per unit mass, $G\mu/(2a_0)$ (with $\mu = m_1m_2/(m_1 + m_2)$ the reduced mass of the binary), becomes greater than the kinetic energy per unit mass of the field stars, $3\sigma^2/2$. This definition of a hard binary gives a critical semi-major axis, $a_H = G\mu/(3\sigma^2)$, which is about 1.8 AU when $m_1 = m_2 = 30M_\odot$ and $\sigma = 50 \text{ km s}^{-1}$. A genuinely hard binary (i.e. one with binding energy $E_{\text{bin}} = 10kT$, with $kT \sim 3\sigma^2/2$ the average thermal energy of stars in the system, see e.g. Heggie & Hut 2003) should have a semi-major axis a_0 about ten times smaller than the above critical value. Hence, for the simulations we consider only $a_0 \leq 0.1 \text{ AU}$.

For each binary we assume a single encounter with an interloper. The reason why we do not consider successive encounters can be seen from Eq. (2): The encounter rate for a HSB binary (of total mass $60M_\odot$ and a semimajor axis of 0.1 AU) with another star is $\sim 5 \cdot 10^{-9} \text{ yr}^{-1}$, while the rate to interact with an HSB interloper is $\sim 5 \cdot 10^{-12} \text{ yr}^{-1}$. I.e. for a Hubble time the binary will interact with 2 stars and with no other HSB.

To first order, the initial mass function (IMF) can be approximated by two well-separated mass scales. We hence consider interlopers of masses $1M_\odot$ (representing within order or magnitude main sequence stars, white dwarfs and neutron stars) and $10M_\odot$ (stellar-mass black holes). The relative abundance (i.e. the number fraction) of objects in these mass ranges after a relaxation time is dominated by the lighter stars (Alexander 2005), and hence we use a number fraction of heavy mass particles of $f_H = 10^{-3} \times f_L$, with f_L the abundance of light stars.

We ran 10^4 samples for each of the experiments to do a statistical study. The code scans different orbital parameters, such as the initial relative velocity and impact parameter, and integrates the system until it has been dynamically solved. This means that the three-body interaction has finished and we are then left with either a new binary with new orbital elements and one of the particles has been ejected, or the binary has coalesced during the three-body interaction because it was set on a very radial orbit and the pericenter was smaller than the semi-major axis defined for coalescence (see below).

We then filter the results looking for binaries that are already in the detector band. For instance, for aLIGO this means that we look for systems with an orbital period of $P_{\text{orb}} \leq 20$ seconds—so that the gravitational wave frequency (the double of the orbital frequency), should be $f_{\text{GW}} \geq 10 \text{ Hz}$. For those systems we calculate the eccentricities at both detector-entrance and coalescence. We assume as a first-order approximation that the systems coalesce if $a = a_{\text{mrg}} := 3R_{\text{Schw}}$, where R_{Schw} is the Schwarzschild radius (for instance, for a $30M_\odot$, $a_{\text{mrg}} \sim 1.8 \cdot 10^{-6} \text{ AU}$).

Even if from a dynamical point of view the three-body interaction has finished before the binary enters the detector band, we want to know how many will be in the detector band within a Hubble time. For this, we evolve the orbital parameters from the last snapshot in the evolution that we have from the numerical code, and we evolve them with an approximation of Keplerian orbits, as in Peters (1964).

The equations evolve a system under the assumption that gravitational radiation is the only source of shrinkage of the semi-major axis of the binary, which is valid in our situation, since we do not allow the binary to interact with any other interloper after the first three-body scattering process. We then evolve them until they reach $f_{\text{GW}} \leq 10$ Hz, provided this happens in within a Hubble time. Of those that enter into the detector band, we record the eccentricity.

The calculations were halted whenever the orbital speed of binary reached $\sim 30\%$ c (the speed of light), since the PN expansion is not valid for higher velocities. Furthermore, once that point in the evolution is reached, the binary will always coalesce. The description of the parameter space of the simulations given below corresponds to that point, which we refer to hereafter as the *merger point* in the evolution of the binary, even if it does not strictly corresponds to the real coalescence of the objects. To speed up calculations, the code analytically treats weakly tidally perturbed binaries: Any hierarchies are analytically treated whenever they are tidally perturbed less than the tidal perturbation tolerance. This means that in a hierarchical triple in which the eccentricity of the outer binary is very large, the inner binary could be treated analytically at each apocenter passage in the orbit—provided it is not strongly tidally perturbed (for more details, see section 3.3.4 of Fregeau et al. 2004). To make this feature work with PN gravity, we added the proviso that a weakly tidally perturbed binary must also have orbital speed at pericenter smaller than $\alpha \cdot c$ to be treated analytically. We typically take $\alpha = 0.05$, which provides a good compromise between accuracy and computational speed.

In Fig. 2 we display the distribution of eccentricities for the scattering experiments at detector entrance. We can readily see that there is a trend towards higher eccentricities as the binary is tighter because the tighter the binary, the shorter the time to coalesce, and the shorter time for GW radiation to reduce the eccentricity. We also explore binaries that initially are more eccentric, as displayed in Figs. (3, 4), initially starting with eccentricities of 0.3, 0.5, 0.7, and 0.9. For these, only a negligible fraction of the experiments with a high initial eccentricity and a very tight semimajor axis achieves a final eccentricity of about ~ 0.1 and a very few events (about 3% of the binaries with initial $e_0 = 0.9$ which are very tight) enter the detector band with $e \sim 0.5$ – 0.7 , to completely circularise a bit before coalescence. All other results stay well below ~ 0.1 . The relative fraction of eccentric binaries is so low that they can be ignored even for the overoptimistic upper limit cases.

Current search strategies are based on templates of circular binaries, so that the size of the parameter space will be manageable. Although this blinds them to most eccentric mergers (Huerta & Brown 2013; Favata 2014), and in principle to the richer information contained in the gravitational wave signals associated with those mergers, these events are so rare that they can be safely ignored. The same applies to field binaries because, as explained before, they will also be circular.

6. DISCUSSION AND CONCLUSIONS

In this work we have addressed the formation channels for BH binaries in the range of observation of ground-based detectors. We find that in the two cases (binaries forming isolated or via dynamical interactions) the most likely is that the binary members are two BHs in the mass range of 30 – $100 M_\odot$, which we call “hyperstellar black holes”, produced by massive WR stars.

We show that the two binary members, again in the two different formation channels, will be slow rotators, meaning a spin magnitude of $a < 0.5$. We show that there is (so far) no possible physical process capable of spinning a HSB up to values $a > 0.5$ in a binary.

We carry out a static study of the eccentricity distribution for a binary of two HSBs in a dense stellar environment. For this we use a numerical Newtonian code in which we have implemented relativistic correcting terms. We prove that HSB binaries will predominantly have almost circular orbits at detector entrance, so that eccentric binaries can be ignored in the searches. Field BH binaries formed in isolation have been shown to also have almost circular orbits at aLIGO frequencies.

Moreover, these binaries should have similar masses. In Section 4 we gave reasons based in relaxation and we referenced as well the work of Miller & Lauburg (2009) for the case of dynamical binaries. Field binaries will also very likely have similar masses, as has been shown with binary evolution and population synthesis codes (de Mink & Belczynski 2015; Dominik et al. 2015).

We therefore predict that HSB binaries will be observed by ground-based detectors with similar masses, low spin magnitudes and almost zero eccentricities, regardless of where they have formed. This has the potential to speed up the searches.

Moreover, a binary of two $30 M_\odot$ BHs, i.e. a HSB binary, will be seen at farther distance than a binary of two $10 M_\odot$ BHs. So the increased volume will ensure that many more massive HSBs will be detected.

Although there is so far no evidence for the existence of HSBs, we deem the non-detection to be related to the limitation of conventional observations in the electromagnetic wavebands. Stellar-origin BHs are discovered whenever a BH is accreting material from a companion star (McClintock et al. 2014). For HSBs, the lifespan in such a configuration is short: The companion star is very likely also a WR star, since they should have similar masses, as we have seen. Since the lifetime of a WR star is only 5 Myr, the time window to observe a HSB binary is very short (even shorter if the two WR stars collapse each to a HSB simultaneously). Hence, HSBs stay virtually always dark in the electromagnetic domain.

With the first detections being imminent, soon the symbiotic relation between astrophysics and data analysis that we mentioned in the introduction will be fulfilled. The upcoming detections will either confirm our prediction or rule it out, and we will hence obtain information about the birth and evolution of stellar black holes, as well as about their environments—information that is virtually inaccessible to our old friend the photon.

We thank Craig Heinke for discussions on observational aspects related to the determination of the spin, and Douglas Hoggie for discussions about binaries. We are thankful to David J. Vanecek for his advice and assistance in C, and Cristián Maureira-Fredes for his help with python. We are indebted with Bruce Allen for granting access to the At-

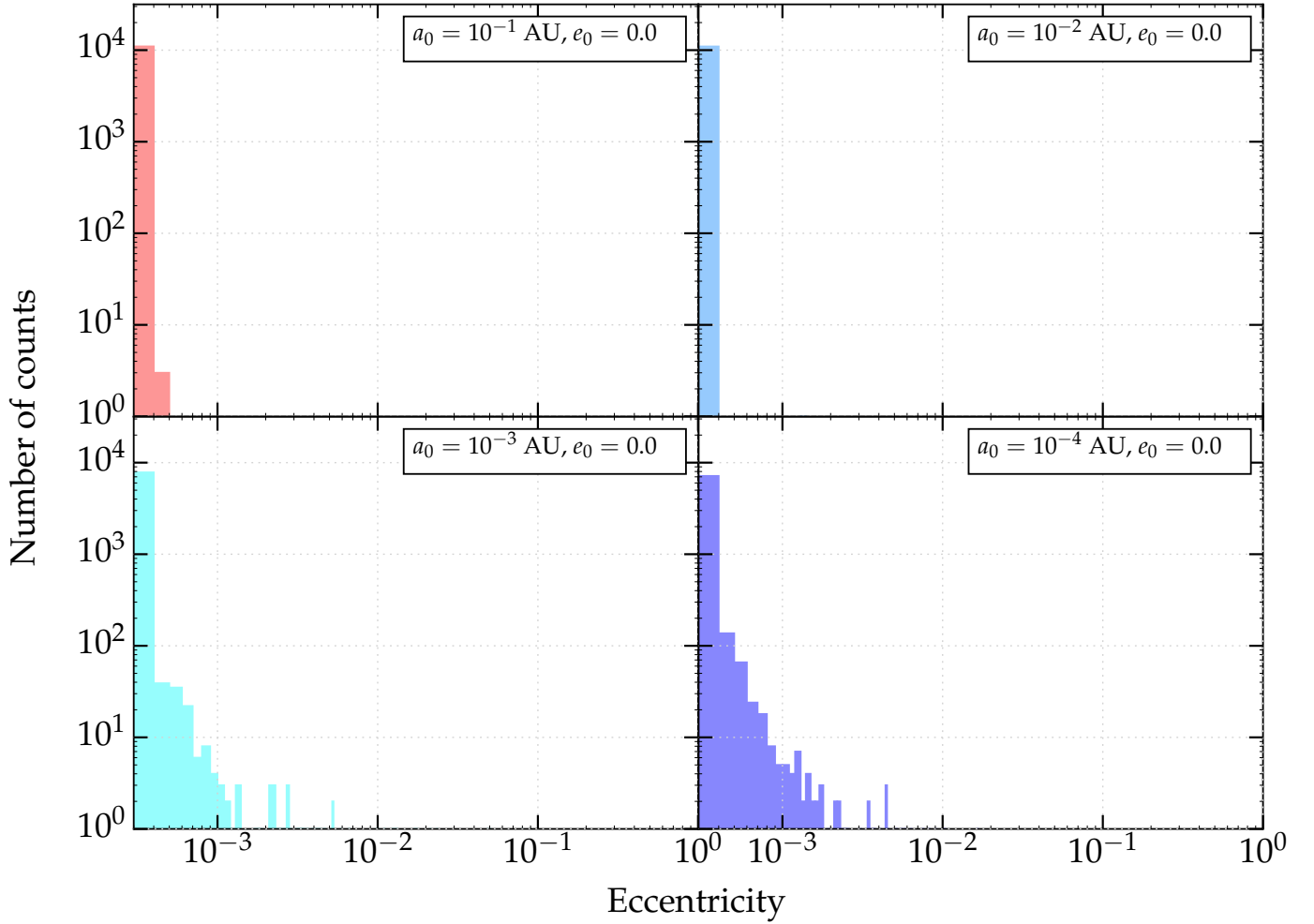


FIG. 2.— Distribution of eccentricities for the binaries described in the text. From the left to the right, top to bottom we show the distribution at detector entrance (aLIGO) for a 10^{-1} , 10^{-2} , 10^{-3} and 10^{-4} AU binary which initially was perfectly circular after interacting with stars in the NSC (for the choice of parameters, see text). The NSC has a velocity dispersion of 50 km s^{-1} .

las cluster, where the simulations were performed, and to Carsten Aulbert for his administration. XC is supported by CONICYT-Chile through Anillo (ACT1101). We thank

Matthew Benacquista for comments on the manuscript. PAS is thankful to Ladislav Šubr and the Astronomical Institute of the Charles University in Prague for a visit, in which this paper was finished.

REFERENCES

- Ajith, P. et al. 2009, 0909.2867
 Alexander, T. 2005, Phys. Rep., 419, 65
 Amaro-Seoane, P., Sopuerta, C. F., & Brem, P. 2012, in European Physical Journal Web of Conferences, Vol. 39, European Physical Journal Web of Conferences, 7001, 1210.6983
 Antognini, J. M., Shappee, B. J., Thompson, T. A., & Amaro-Seoane, P. 2014, MNRAS, 439, 1079
 Antonini, F., Chatterjee, S., Rodriguez, C. L., et al. 2015, arXiv:1509.05080
 Antonini, F., Murray, N., & Mikkola, S. 2014, ApJ, 781, 45
 Baker, J. G., Boggs, W. D., Centrella, J., Kelly, B. J., McWilliams, S. T., Miller, M. C., & van Meter, J. R. 2008, ApJ, 682, L29
 Baker, J. G., Centrella, J., Choi, D.-I., Koppitz, M., & van Meter, J. 2006, Phys. Rev. Lett., 96, 111102
 Belczynski, K., Kalogera, V., Rasio, F. A., et al. 2008, ApJS, 174, 223
 Belczynski, K., Repetto, S., Holz, D., O’Shaughnessy, R., Bulik, T., Berti, E., Fryer, C., & Dominik, M. 2015, ArXiv e-prints
 Benacquista, M. J., & Downing, J. M. B. 2013, Living Reviews in Relativity, 16, 4
 Blaes, O., Lee, M. H., & Socrates, A. 2002, ApJ, 578, 775
 Blanchet, L., & Iyer, B. R. 2003, Classical and Quantum Gravity, 20, 755
 Böker, T. 2010, IAU Symposium, 266, 58
 Brem, P., Amaro-Seoane, P., & Sopuerta, C. F. 2014, MNRAS, 437, 1259
 Brem, P., Amaro-Seoane, P., & Spurzem, R. 2013, MNRAS, 434, 2999
 Brown, D. A., Kumar, P., & Nitz, A. H. 2013, Ph. Rv. D, 87, 082004
 Buonanno, A., & Damour, T. 1999, Phys. Rev. D, 59, 084006
 Buonanno, A., Pan, Y., Baker, J. G., Centrella, J., Kelly, B. J., McWilliams, S. T., & van Meter, J. R. 2007, Phys. Rev. D, 76, 104049
 Campanelli, M., Lousto, C. O., Marronetti, P., & Zlochower, Y. 2006, Phys. Rev. Lett., 96, 111101
 de Mink, S. E., & Belczynski, K. 2015, ApJ, 814, 58
 Dominik, M. et al. 2015, ApJ, 806, 263
 Favata, M. 2014, Phys. Rev. Lett., 112, 101101
 Fregeau, J. M., Cheung, P., Portegies Zwart, S. F., & Rasio, F. A. 2004, MNRAS, 352, 1
 Fregeau, J. M., & Rappaport, S. A. 2004, in preparation
 Fryer, C. L., Belczynski, K., Wiktorowicz, G., Dominik, M., Kalogera, V., & Holz, D. E. 2012, ApJ, 749, 91
 Heger, A., Fryer, C. L., Woosley, S. E., Langer, N., & Hartmann, D. H. 2003, ApJ, 591, 288
 Heggie, D., & Hut, P. 2003, The Gravitational Million-Body Problem: A Multidisciplinary Approach to Star Cluster Dynamics, by Douglas Heggie and Piet Hut. Cambridge University Press, 2003, 372 pp.
 Hirschi, R., Meynet, G., & Maeder, A. 2005, A&A, 443, 581
 Huerta, E. A., & Brown, D. A. 2013, Phys.Rev.D, 87, 127501
 Kupi, G., Amaro-Seoane, P., & Spurzem, R. 2006, MNRAS, L77+
 LIGO Scientific Collaboration et al. 2013, ArXiv e-prints

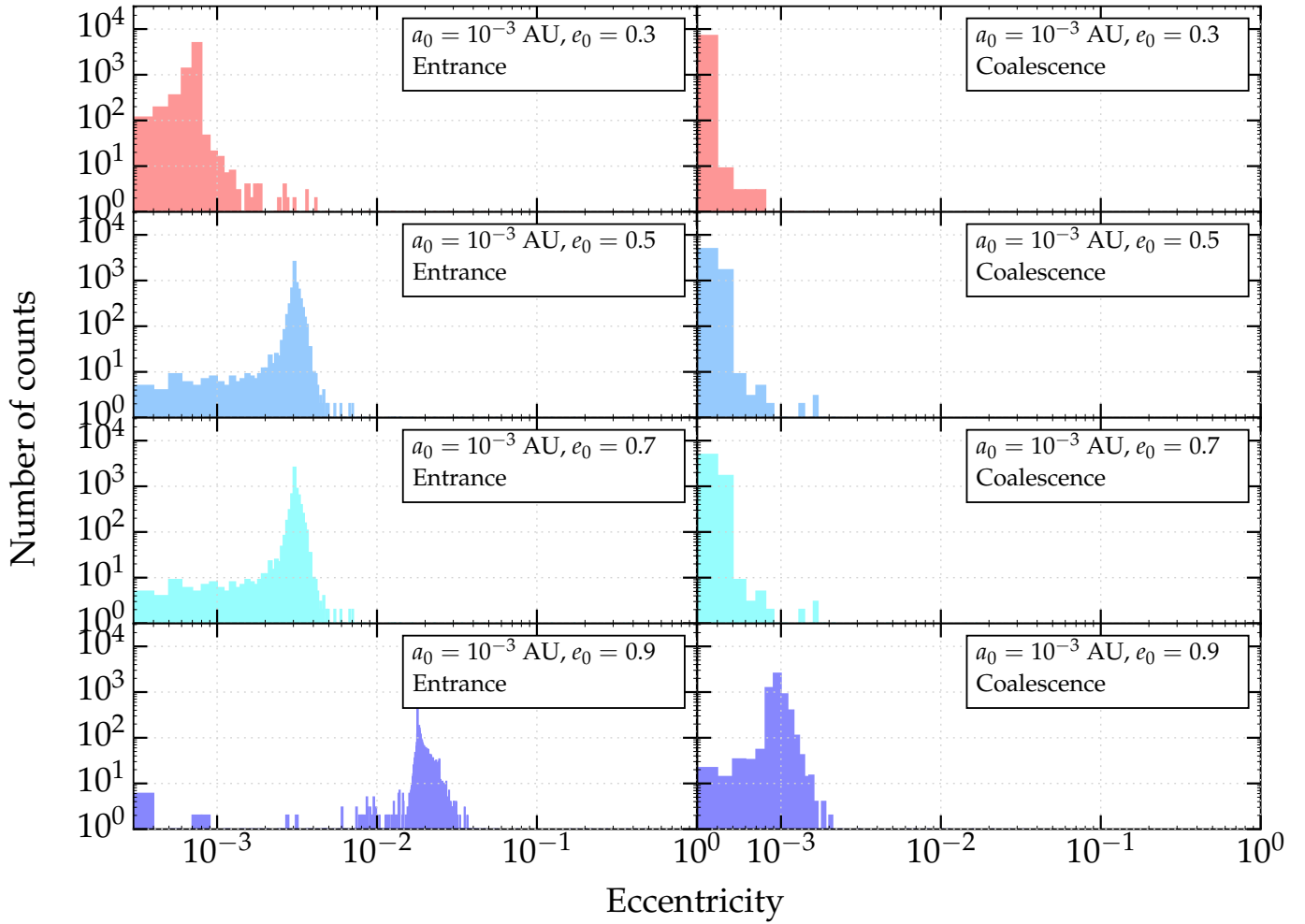


FIG. 3.— Same as Fig. (2) but for a 10^{-3} AU binary and four different initial eccentricities of 0.3, 0.5, 0.7 and 0.9 from the top to the bottom, at detector entrance (left panels) and just before coalescence (right panels), see text.

Liu, F. K., Wang, D., & Chen, X. 2012, *ApJ*, 746, 176
 Mapelli, M., Colpi, M., & Zampieri, L. 2009, *MNRAS*, 395, L71
 Mapelli, M., Ripamonti, E., Zampieri, L., Colpi, M., & Bressan, A. 2010, *MNRAS*, 408, 234
 Mapelli, M., Zampieri, L., Ripamonti, E., & Bressan, A. 2013, *MNRAS*, 429, 2298
 Mapelli, M., & Zampieri, L. 2014, *ApJ*, 794, 7
 McClintock, J. E., Narayan, R., & Steiner, J. F. 2014, *Space Science Reviews*, 183, 295
 Meynet, G., & Maeder, A. 2003, *A&A*, 404, 975
 —. 2005, *A&A*, 429, 581
 Miller, M. C., & Hamilton, D. P. 2002, *ApJ*, 576, 894
 Miller, M. C., & Lauburg, V. M. 2009, *ApJ*, 692, 917
 O’Leary, R. M., Rasio, F. A., Fregeau, J. M., Ivanova, N., & O’Shaughnessy, R. 2006a, *ApJ*, 637, 937
 —. 2006b, *ApJ*, 637, 937
 Panter, B., Jimenez, R., Heavens, A. F., & Charlot, S. 2008, *MNRAS*, 391, 1117
 Peters, P. C. 1964, *Physical Review*, 136
 Pretorius, F. 2005, *Phys. Rev. Lett.*, 95, 121101

Rezzolla, L., Barausse, E., Dorband, E. N., Pollney, D., Reisswig, C., Seiler, J., & Husa, S. 2008, *Phys. Rev. D*, 78, 044002
 Rodriguez, C. L., Morscher, M., Pattabiraman, B., Chatterjee, S., Haster, C.-J., & Rasio, F. A. 2015, *Physical Review Letters*, 115, 051101
 Santamaría, L. et al. 2010, *Phys Rev D*, 82, 064016
 Sathyaprakash, B. S., Schutz, B. F., & Van Den Broeck, C. 2010, *Classical and Quantum Gravity*, 27, 215006
 Strader, J., Chomiuk, L., Maccarone, T. J., Miller-Jones, J. C. A., & Seth, A. C. 2012, *Nature*, 490, 71
 van Meter, J. R., Miller, M. C., Baker, J. G., Boggs, W. D., & Kelly, B. J. 2010, *ApJ*, 719, 1427
 Wen, L. 2003, *ApJ*, 598, 419
 Woosley, S. E., Heger, A., & Weaver, T. A. 2002, *Reviews of Modern Physics*, 74
 Yusof, N., Hirschi, R., Meynet, G., et al. 2013, *MNRAS*, 433, 1114
 Zinnecker, H., & Yorke, H. W. 2007, *A&A*, 45, 481
 Ziosi, B. M., Mapelli, M., Branchesi, M., & Tormen, G. 2014, *MNRAS*, 441, 3703

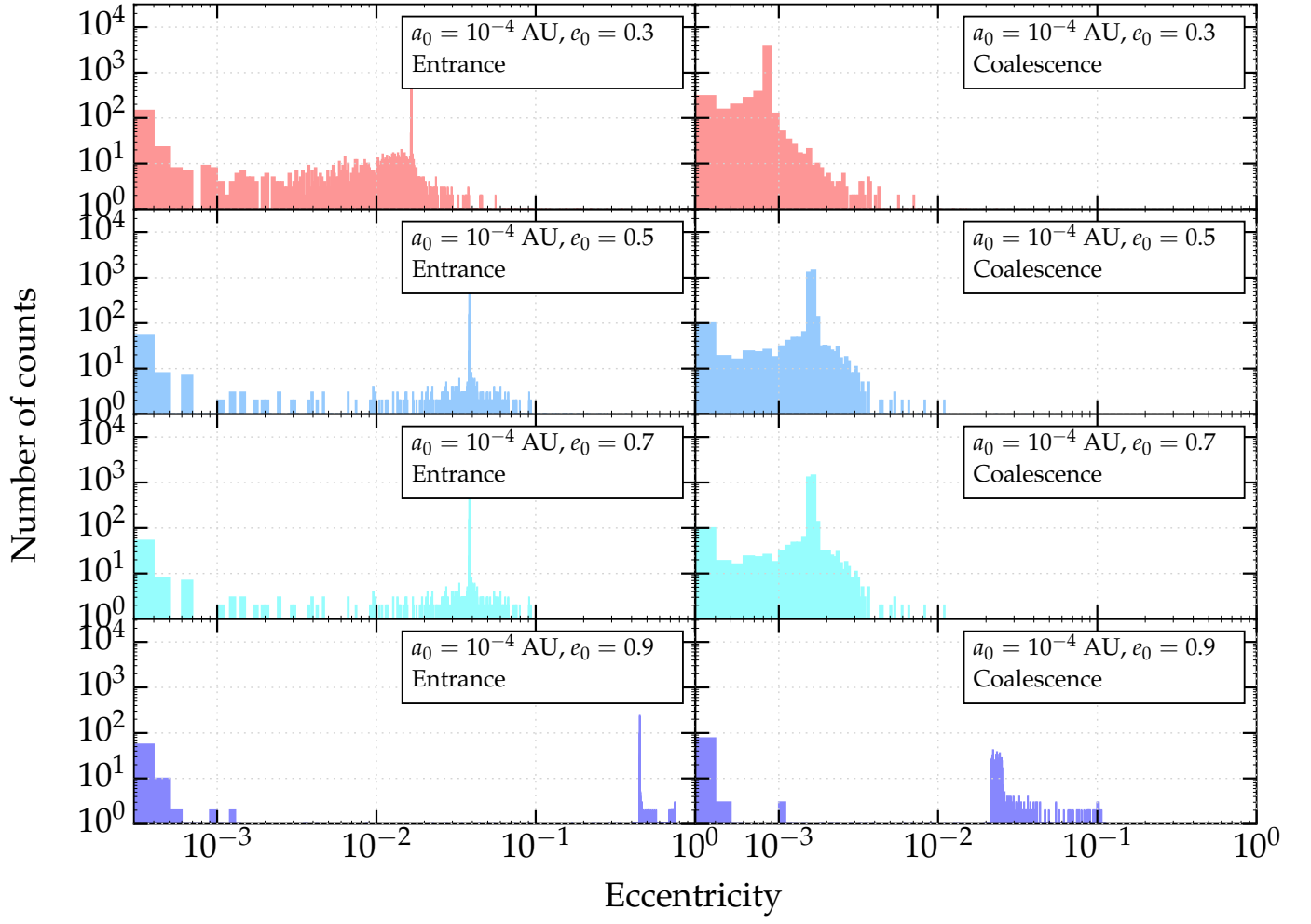


FIG. 4.— Same as Fig. (3) but for a 10^{-4} AU binary.